DIRECTIONAL MECHANICAL PROPERTIES OF RADIATION RECRYSTALLIZED SNOW LAYERS FROM EXPERIMENTAL TESTING

David J. Walters*
Edward E. Adams
Montana State University, Bozeman, Montana

Snow's microstructure is a large factor in the determination of its mechanical characteristics. The process of radiation recrystallization creates a particular microstructure that exhibits distinct directional differences in its mechanical properties. Using meteorological conditions associated with radiation recrystallized snow obtained from the field, such layers have been produced in a laboratory setting. Shear and compression testing of uniform samples prior to laboratory induced metamorphism provide baseline results for investigating departures away from uniform mechanical properties when a faceted layer develops. A procedure based on bond contact orientation is used to describe the configuration or "fabric" of the microstructure. This is used in conjunction with the pair of mechanical tests to describe the degree of directional dependence of the radiation recrystallized layer. Mechanical testing in compression indicates that radiation recrystallization results in an increase in the stiffness perpendicular to the snow surface. Shear testing indicates a decrease in shear stiffness parallel to the snow surface when compared to the isotropic material properties. Importantly, both shear strength and compressive strength were reduced following radiation recrystallization metamorphism.

1. INTRODUCTION

Comprehensive mechanical testing for properties of uniformly structured snow has been performed and compiled in several places (e.g. Mellor(1975), Föhn (1998), Schweizer (1999), and Stoffel (2005)). An area lacking detail is directional properties for non-uniformly structured snow. In this study, the growth and mechanical testing of radiation recrystallized facets are addressed.

Radiation recrystallized snow is composed of faceted snow crystals that are formed by crystal growth within the existing snow structure caused by near surface temperature gradients (Colbeck, 1989). These temperature gradients develop as a result of subsurface warming from incoming shortwave radiation and surface cooling due to outgoing longwave radiation (Colbeck, 1989). More recent investigations of radiation recrystallization have identified conducive conditions for radiation recrystallization and procedures for reproducing these faceted layers in a laboratory setting (Morstad, 2004; Morstad et al., 2004; Morstad et al., 2007; Slaughter et al., 2011; Slaughter et al., 2009; Slaughter et al., 2008). A case study by Birkeland (1998) indicated near-surface facet layers (which included radiation recrystallization) accounted for 59% of avalanches in southwest Montana, USA between 1990-91 and 1995-96.

Temperature gradient induced metamorphism in snow containing predominantly rounded grains results in a change from rounded and fragmented grained snow with uniform properties to a structure with distinct directional material properties (Kry, 1975; Schneebeli and Sokratov, 2004; Srivastava et al., 2010; Sturm et al., 1997). In particular, radiation recrystallized snow contains uniform properties in the X_1 and X_3 directions and independent properties in the X_2 directions (see Figure 1).

* *Corresponding author address:*
David J. Walters, Civil Engineering,
Montana State University, 205 Cobleigh Hall,
Bozeman, MT 59717-3900; tel: 406-994-2293;
Email: david.walters@ce.montana.edu

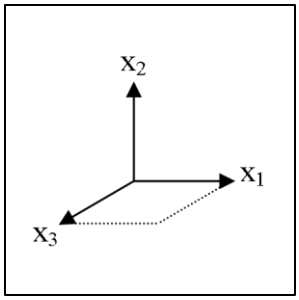

Figure 1: Global coordinate system used for all directional quantities. For the transversely isotropic structure, the X_2 axis is the independent axis and the plane defined by X_1 and X_3 is the isotropic plane.

A mathematical quantity called a contact tensor used to describe the relative difference between directional properties was developed for snow by Shertzer (2011) and Shertzer and Adams (2011) and analyzed using Computed Tomography (CT). The tensor quantities are estimated in this paper from the results of separate shear and compressive mechanical tests. Shear tests are performed to investigate the shear modulus. The shear modulus is a material property dictating the shear stiffness or the amount of force required to shear a sample from its original configuration. Compressive tests are performed to measure the Young's modulus, which pertains to the axial stiffness of a material. To obtain deformation data of mechanically loaded snow samples, an optical strain measuring system is employed. This device is conceptually similar to the Particle Image Velocimetry (PIV) used by Gleason (2006) and more recently, Reiweger et al. (2010), however, it achieves a faster capture rate (up to 15 frames per second) and higher resolutions (Walters et al., 2010). The hypothesis is that quantifiable departures from uniform material properties develop as radiation recrystallized snow departs from a uniform structure.

2. RADIATION RECRYSTALLIZATION

Conditions required for radiation recrystallization of a snow surface are obtained from observations made at meteorological field stations located on Pioneer Mountain in the Central Madison Mountains in Southwest Montana. Field operations at this location are detailed by McCabe et al. (2008), Slaughter et al. (2009), Slaughter (2010), and Slaughter et al. (2011). One day was selected to provide representative conditions for laboratory experiments

Conditions conducive for radiation recrystallized facet formation were observed on 3 January, 2011 and produced near surface facets. Facets of 0.5 mm were observed (Figure 2). Previously, 2.5 cm of new snow had fallen overnight with about 7.5 cm of new snow in the preceding 24 hours. The facets formed on 0.5 mm decomposing stellar crystals resulting from the new snow overnight. By 1330, when the observation was made, incoming shortwave radiation peaked near 1,000 W/m^2. Incoming longwave radiation varied between 215 and 315 W/m^2. The ambient air temperature rose to -6.5 °C from -16°C before sunrise.

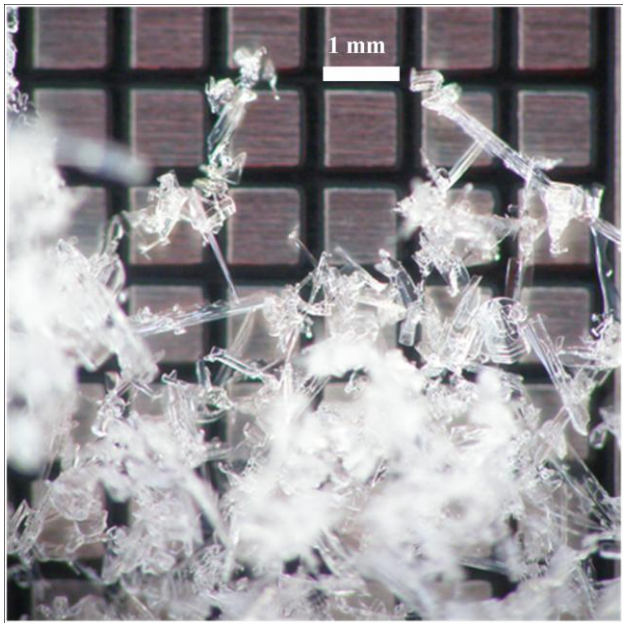

Figure 2: Surface facets resulting from radiation recrystallization observed at 1330 on 3 January, 2011 at the south field station on Pioneer Mountain. Crystals were disaggregated from the snowpack (photo, D. McCabe, Yellowstone Club Ski Patrol).

These conditions were used for an environmental chamber at the Subzero Science and Engineering Facility (SSERF) at Montana State University. The incoming longwave radiation is predominantly

controlled by the temperature of the independently controlled chamber ceiling. Shortwave radiation is provided by a metal-halide luminary.

Before meteorological conditions are applied, the snow samples must be prepared. Fragmented dendritic crystals are produced in the laboratory using a snow breeder which transports moist air past nucleation sites. As crystals accumulate, they are collected. The top 10 cm of the sample are sieved through a 0.7mm grid to produce uniform crystal sizes around 0.5 to 0.7 mm oriented randomly to build an isotropic structure (after short term settling affects have slowed). This technique, when employed with the laboratory produced snow, results in densities ranging from 150-250 kg/m^3.

After the snow sample is prepared, instrumentation is mounted to the sample box to collect pertinent meteorological conditions. Snow surface temperatures are recorded with an Everest Interscience Inc. 4000.4ZL infrared thermometer. All other temperature measurements are recorded using type T thermocouples including a 10cm array of thermocouples spaced 1cm vertically for measuring temperature gradients near the surface of the snow. Incoming shortwave and longwave radiation is read via an Eppely Labs Precision Spectral Pyranometer and an Eppely Labs Precision Infrared Radiometer respectively. For this experiment, incoming shortwave intensity of approximately 850 W/m^2 and incoming longwave radiation between 220 and 320 W/m^2 were achieved. Experiments are subjected to these conditions for 12-15 hours.

Initially, the ambient air temperature and snow sample are maintained at -15°C. As shortwave radiation is applied to the sample, local air temperatures near the snow surface increase to a steady state of -8 to -5°C as a result of shortwave radiation interaction with the snow. The resulting temperature cycle of the experiment follows a similar temperature cycle observed 3 January, 2011.

3. LABORATORY PROCEDURES

Before and after laboratory induced radiation recrystallization, samples are mechanically tested using identical procedures. Mechanical testing is implemented by loading a 256 cm^2 load frame using displacement rate control. This frame can be loaded directly in shear and, when capped, can be loaded in compression.

Initially a covered sample is brought to -15°C and allowed to sinter. Before manipulating a sample containing a radiation recrystallized surface, the solar source is switched off to allow the snow to equilibrate at -15°C.

New snow is then added incrementally from the same source as the original. A layer is sieved 10 mm thick and allowed to rest 15 to 20 minutes to allow additional sintering to take place so the weight of the frame can be supported when placed atop the surface. The empty space inside the frame is filled by sieving snow until it covers the top of the frame. A schematic of this setup is shown with the presence of a faceted layer in Figure 3. The faceted layer is omitted when testing without a faceted layer. To allow the new snow to achieve the same properties as the original snow, the setup is allowed to rest for 6 or more hours to allow sintering of the snow around the frame to take place.

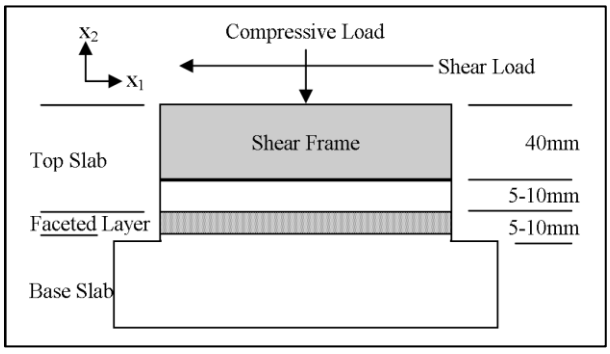

Figure 3: Schematic profile of the snow layering during setup for a mechanical shear test. For a test involving a sample absent of a radiation recrystallized layer, the area depicted as the "faceted layer" is omitted from the schematic.

During the resting period for sintering, a load actuator and alignment assembly is attached to the snow sample box. The load actuator, a GeoTac – GeoJac soils testing apparatus, is modified for use with this experiment (Walters et al., 2010). It is mounted in a frame which allows for modifying the load angle between 0° (horizontal shear loading) and 90° (vertical compression loading). Once the framing is mounted to the snow sample box, the load angle and alignment of the actuator is set.

Next, the snow sample inside the frame is isolated and prepared for mechanical testing and analysis. Excess snow from the top is removed so that a cap used for compressive loading can be placed. Following this, excess snow from the outside of the frame is removed. Snow is removed from all 4 sides slightly deeper than the original snow interface. The column is kept short to minimize the bending moment imparted by the shear loading setup in which the shear load is applied near the top of the column. Snow is removed slightly deeper than the interface of interest to avoid creating stress concentrations that may undesirably affect the outcome of the test.

Once this is done, the side facing the outside of the snow box is cut well below the bed surface described above to provide a smooth vertical face suitable for analysis by a GOM-ARAMIS optical strain measuring system. This system, containing a pair of cameras and supporting software, obtains a stereological 3-D mapping of the surface by tracking an applied contrasting speckle pattern to measure displacement and strain of the exposed face. Accuracy of ARAMIS measurements are determined from signal noise pattern in individual tests. Accuracy in the tests discussed here varied from 10-20 μm.

After the ARAMIS system is calibrated and aligned, and the snow column prepared, mechanical testing is initiated. Loading on the GeoTac – GeoJac system for these experiments are set to displacement rate of 0.1mm/s for both shear and compressive tests. With an average sample height of 50mm, this gives a compressive strain rate of $2 \times 10^{-3} \mathrm{s}^{-1}$ which is in accordance with elastic strain rates tested by Schweizer (1998) and Reiweger et. al (2010). Once baseline results are established for a sample without a faceted layer, the sample undergoes radiation recrystallization and is mechanically tested again. The pair of mechanical tests makes up one complete set in which the changes in elastic material properties following radiation recrystallization are observed.

4. RESULTS AND ANALYSES

Shear and compression test results are summarized below. Shear tests were performed on samples 1 through 4, and compression tests were performed on samples 5 through 8. In all samples, the stress-strain curves were linear from the start until sample failure, indicating brittle failure.

The shear modulus (shear stiffness) before and after radiation recrystallization is denoted by μ^{iso} and μ^{rr} respectively. The Young's modulus (axial stiffness) before and after radiation recrystallization is denoted by E^{iso} and E^{rr} respectively.

4.1 Shear Tests

Sample 1 had an initial density of approximately 230 kg/m^3 for an ice volume fraction of 0.251. Following shear testing on the non-layered sample, the shear modulus of the isotropic plane, μ^{iso} was measured as 1.51 MPa. Since a clear failure plane was not present, the shear strength, τ_s^{iso}, was greater than 2.66 kPa in the plane of the applied direct shear. Following the same testing on the sample after radiation recrystallization produced a layer of surface facets, the shear modulus of the isotropic plane, μ^{rr} was calculated as 1.31 MPa with a shear strength, τ_s^{rr}, of 0.406 kPa. This is a 13.2% reduction in shear stiffness and at least an 85% reduction in shear strength from the isotropic, non-layered sample. The plotted strain field produced by ARAMIS allows for isolation of the radiation recrystallized layer for analysis. The region of the weak layer is

detectable in Figure 4 by the blue region showing significant local shear straining.

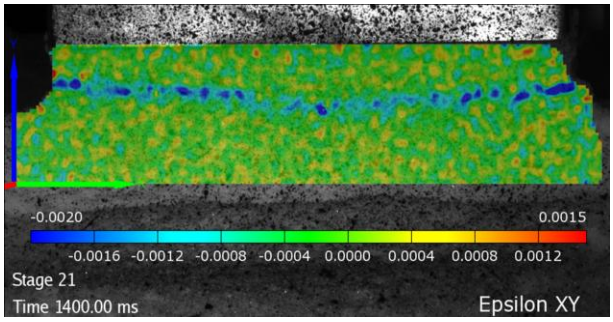

Figure 4: Shear strain of sample 1 containing a faceted layer 66.7 ms before total failure of the faceted layer occurs. The location of the faceted layer is easily seen as a line of local shear straining stretched horizontally across the figure. The shear load is applied right to left across the top of the sample.

Similar results for the remaining shear tests are reported in Table 1. It is difficult to compare relative changes in shear strength since the baseline tests did not fail with a clean shear plane. The test setup described previously does not guarantee shear failure, especially in uniform columns not containing a faceted layer.

Table 1: Material properties given for the isotropic configuration and faceted configuration following radiation recrystallization and shear testing. In these tests, $\boldsymbol{\mu^{iso}}$ and $\boldsymbol{\mu^{rr}}$ are measured parallel to the snow surface.

	ρ_{snow} kg m^{-3}	μ^{iso} MPa	μ^{rr} MPa	τ_s^{no} kPa	τ_s^{rr} kPa
1	230	1.51	1.31	>2.66	0.406
2	154	0.438	0.372	>1.18	1.43
3	205	0.509	0.451	>2.34	1.98
4	235	1.55	1.27	>2.43	1.27

4.1 Compression Tests

Sample 5 had an initial density of 190 kg/m^3 or an ice volume fraction of 0.207. The uniform sample subjected to compressive loading produced a compressive Young's modulus along the vertical axis, E^{iso}, of 1.24 MPa and a compressive strength, σ_s^{iso}, of 1.96 kPa. Following radiation recrystallization of the surface which produced a layer of surface facets, compressive testing showed an increase in Young's modulus along the independent axis, E^{rr}, and a decrease in compressive strength, σ_s^{rr}, to 1.11 kPa. A summary of material properties for sample 5 are in Table 2.

Calculation of Young's modulus on only the faceted layer was more difficult. Unlike the shear case in Figure 4 where the location of the faceted layer is easily visible, the location and thickness of the faceted layer is not apparent in images taken during the compression test until after failure of the sample. Instead, the Young's modulus reported is an average of the observed modulus across an estimated cross section height. Using the smallest cross-section height known to contain the faceted layer, a Young's modulus of 5.94 MPa was measured resulting in an increase of 379% over the isotropic case.

Similar results for the remaining compression tests are reported in Table 2.

Table 2: Material properties given for the isotropic configuration and faceted configuration following radiation recrystallization and compression testing. In these tests, $\boldsymbol{E^{iso}}$ and $\boldsymbol{E^{rr}}$ are measured perpendicular to the snow surface.

	ρ_{snow} kg m^{-3}	E^{iso} MPa	E^{rr} MPa	σ_s^{no} kPa	σ_s^{rr} kPa
5	190	1.24	5.94	1.96	1.11
6	180	1.03	3.47	2.52	1.00
7	150	0.784	2.09	1.51	1.67
8	147	1.12	3.91	5.00	5.31

5. DISCUSSION

Change in the material properties from radiation recrystallization is evident in the shear and compression tests. Test results assume stress and strain measurements are taken within the elastic load range on each sample. From shear tests, the average decrease in measured shear modulus parallel to the snow surface, μ, in the faceted snow was approximately 14% following radiation recrystallization. Compression tests resulted in an average measured increase in the Young's modulus perpendicular to the surface of 258%. Associating changes in shear behavior with changes in axial behavior requires the data to be comparable on the same scale. To compare the relative changes observed in shear tests and compressive tests, the contact tensor is employed to allow direct comparison of two different mechanical tests.

The contact tensor provides a mathematical representation of how the individual grains in snow are bonded together. Shertzer's (2011) and Shertzer's and Adams' (2011) method for determining the coefficients of the contact tensor uses CT imagery to directly compute the distribution of bond orientations. The resulting contact tensor is represented with this 3x3 matrix:

$$F = \begin{bmatrix} F_{11} & 0 & 0 \\ 0 & F_{22} & 0 \\ 0 & 0 & F_{33} \end{bmatrix}. \qquad (1)$$

Each coefficient of the matrix represents the probability of finding a bond oriented in the associated coordinate direction (from Figure 1). Since each coefficient is a probability, the sum of the diagonal values is always one.

When a sample contains a random microstructural configuration, it is assumed the rounded and decomposing grains have a uniform distribution of inter-grain bond plane orientations. From the contact tensor point of view, this configuration is reflected by having equal tensor coefficients along its diagonal of the coefficient matrix, meaning there is a uniform probability distribution of bond plane orientations across all directions. In Figure 5, this value is approximately 1/3 (shown by the red line) since the sum of the coefficients must be one. Physically, this means a load applied from any of the three directions garners the same mechanical response.

Following radiation recrystallization, it is presumed the resulting faceted crystals grow with bond planes preferentially orienting with the driving temperature gradient. This implies that most vectors between the centers of bonded ice grains are oriented parallel to the temperature gradient. When the distribution of bond plane directions diverge from a uniform distribution as shown in Figure 5 following radiation recrystallization, the values of the contact tensor give information regarding the preferred direction of bond

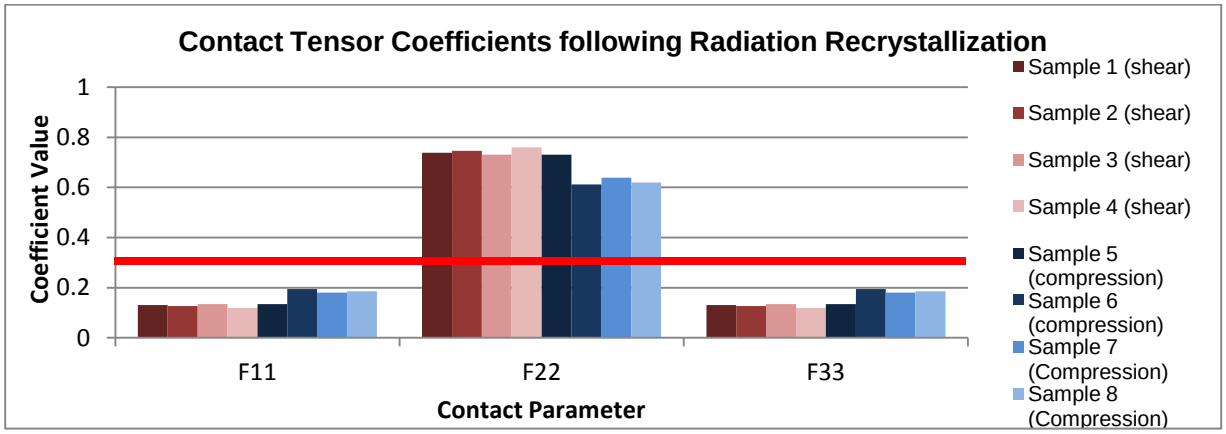

Figure 5 Contact tensor coefficients of the radiation recrystallized snow resulting from shear and compression tests as indicated. The red line indicates the isotropic/random configuration values of the contact tensor.

orientations.

In addition, Shertzer (2011) proposes a relationship between mechanical stiffness and the contact tensor. The shear modulus parallel to the snow surface is related by:

$$\mu^{rr} = \mu^{iso}\left(\frac{[F_{11}F_{22}]^{rr}}{9}\right). \qquad (2)$$

Young's modulus in the vertical direction is related by:

$$\frac{1}{E^{rr}} = \frac{1}{E^{iso}}\left(\frac{1}{3F_{22}^{rr}}\right)^2, \qquad (3)$$

Following compressive testing, both the isotropic and radiation recrystallized Young's moduli (E^{iso} and E^{rr}) are known. Equation 3 can be used to determine the change in contact tensor coefficients. A similar procedure is followed using Equation 2 if shear testing was performed. After calculating the coefficients for each sample, the results are plotted in Figure 5.

6. CONCLUSIONS

Radiation recrystallized facets can be formed under laboratory conditions with similar physical characteristics as those found in the field. Laboratory mechanical testing on uniform and radiation recrystallized snow show the faceting process results in a large increase in vertical stiffness and a decrease in shear stiffness.

In addition, experimental testing showed a reduction in compressive strength in two compression tests as a result of radiation recrystallization, and a reduction in shear strength in three of the tests.

7. ACKNOWLEDGEMENTS

This research was supported by the US National Science Foundation (NSF) grant No. 1014997. The Montana State University Subzero Science and Engineering Facility was funded by the NSF and the M.J. Murdock Charitable Trust under two separate grants. We also thank the Yellowstone Club for providing access, resources, and data collection/photography.

8. REFERENCES

Birkeland, K., 1998. Terminology and predominat processes associated with the formation of weak layers of near-surface faceted crystals in the mountain snowpack. Arctic and Alpine Research, 30(2): 193-199.

Colbeck, S., 1989. Snow-crystal growth with varying surface temperatures and radiation penetration. Journal of Glaciology, 35(119): 23-39.

Föhn, P.M.B., Camponovo, C. and Krüsi, G., 1998. Mechanical and structural properties of weak snow layers measured in situ. Annals of Glaciology, 26: 1-6.

Gleason, A., 2006. Particle image velocimetry: A new technique to measure strain in loaded snow. The Avalanche Review, 24(3): 12.

Kry, P.R., 1975. Quantitative stereological analysis of grain bonds in snow. Journal of Glaciology, 14(72): 467-477.

McCabe, D., Munter, H., Catherine, D., Henninger, I., Cooperstein, M., Leonard, T., Adams, E.E., Slaughter, A.E. and Staron, P.J., 2008. Near-Surface Faceting on South Aspects in Southwest Montana, International Snow Science Workshop, Whistler, British Columbia, Canada, pp. 147-154.

Mellor, M., 1975. A review of basic snow mechanics, The International Symposium on Snow Mechanics, Grindelwald, Switzerland, pp. 251-291.

Morstad, B.W., 2004. Analytical and Experimental Study of Radiation-Recrystallized Near-Surface Facets in Snow, Montana State University, Bozeman, Montana, USA, 204 pp.

Morstad, B.W., Adams, E.E. and McKittrick, L.R., 2004. Experimental study of radiation-recrystallized near-surface facets in snow, International Snow Science Workshop, Jackson Hole, WY.

Morstad, B.W., Adams, E.E. and McKittrick, L.R., 2007. Experimental and Analytical Study of radiation-recrystallized near-surface facets in snow. Cold Regions Science and Technology, 47(1-2): 90-101.

Reiweger, I., Schweizer, J., Ernst, R. and Dual, J., 2010. Cold Regions Science and Technology Load-controlled test

apparatus for snow. Cold Regions Science and Technology, 62(2-3): 119-125.

Schneebeli, M. and Sokratov, S.A., 2004. Tomography of temperature gradient metamorphism of snow and associated changes in heat conductivity. Hydrological Processes, 18: 3655-3665.

Schweizer, J., 1998. Laboratory experiments on shear failure of snow. Annals of Glaciology, 26: 97-102.

Schweizer, J., 1999. Review of dry snow slab avalanche release. Cold Regions Science and Technology, 30(1-3): 43-57.

Shertzer, R., 2011. Fabric tensors and effective properties of granular materials with applications to snow, Montana State University, Bozeman.

Shertzer, R.H. and Adams, E.E., 2011. Anisotropic Thermal Conductivity Model for Dry Snow. Cold Regions Science and Technology, 69(2-3): 122-128.

Slaughter, A.E., 2010. Numerical analysis of conditions necessary for near-surface snow metamorphism, Montana State Universityq, Bozeman, Montana, USA, 461 pp.

Slaughter, A.E., Adams, E.E., Staron, P.J., Shertzer, R.H., Walters, D.J., McCabe, D., Catherine, D., Henninger, I., Leonard, T., Cooperstein, M. and Munter, H., 2011. Field investigation of near-sruface metamorphism of snow. Journal of Glaciology, 57(203): 441-452.

Slaughter, A.E., McCabe, D., Munter, H., Staron, P.J., Adams, E.E., Catherine, D., Henninger, I., Cooperstein, M. and Leonard, T., 2009. An investigation of radiation-recrystallization coupling laboratory and field studies. Cold Regions Science and Technology, 59(2-3): 126-132.

Slaughter, A.E., Staron, P.J., Adams, E.E., McCabe, D., Munter, H., Catherine, D., Henninger, I., Cooperstein, M. and Leonard, T., 2008. Laboratory simulations of radiation-recrystallization events in southwest montana, International Snow Science Workshop, Whistler, British Columbia, CANADA, pp. 139-146.

Srivastava, P.K., Mahajan, P., Satyawali, P.K. and Kumar, V., 2010. Observation of temperature gradient metamorphism in snow by X-ray computed microtomography: measurement of microstructure parameters and simulation of linear elastic properties. Annals of Glaciology, 50(54): 73-82.

Stoffel, M., 2005. Numerical Modelling of Snow Using Finite Elements. Dissertation Thesis, Swiss Federal Institute of Technology Zurich, Zurich, 142 pp.

Sturm, M., Holmgren, J., Konig, M. and Morris, K., 1997. The thermal conductivity of seasonal snow. Journal of Glaciology, 43(143): 26-41.

Walters, D.J., Adams, E.E., Staron, P.J. and McKittrick, L.R., 2010. Shear deformation of radiation recrystallized near surface facets, International Snow Science Workshop, Lake Tahoe, CA, USA.